DOI:
10.1039/C6SM01774F

Document Version
Peer reviewed version

Soft Matter

ARTICLE TYPE

Cite this: DOI: 10.1039/xxxxxxxxxx

On demand modulation of lipid composition in an individual bilayer†

John S. H. Danial,[a‡] Bríd Cronin,[a] Chandini Mallik,[a] and Mark I. Walllace.*[a,b]

Received Date
Accepted Date

DOI: 10.1039/xxxxxxxxxx

www.rsc.org/journalname

Changes in local lipid composition are thought to play a key role in regulating many complex cellular processes. By studying lipid organization in artificial lipid bilayers the physical principles underlying these process can be studied in detail. However, such *in vitro* measurements are often hindered by heterogeneities in the lipid composition of individual bilayers prepared by current bulk methods. Here, the lipid composition of an individual Droplet Interface Bilayer is varied by lipid titration into the bilayer from the oil phase in a microfluidic device. Control of lipid composition allows the reversible switching between single- and two-phase regions and sampling of specific lipid compositions in an individual bilayer. This method enables controlled modulation of composition-sensitive processes in a single lipid membrane.

Introduction

The intrinsic modulation of lipid composition in cells exerts profound and complicated influences on their organization [1–3]. Artificial lipid bilayers have helped us understand how phase separation occurs in lipid membranes, reducing membrane complexity down to a small number of well-defined components whose properties can be predicted [4–6]. Giant Unilamellar Vesicles (GUVs) in particular have been used to study lipid phase separation; mapping out phase diagrams [7,8] and investigate the dynamics of lipid domains [9–11].

Despite their usefulness, phase separated GUVs show significant variations in their transition temperature and area fraction within the same preparation [9,12,13]; similar inhomogeneity has also been recently reported for small unilamellar vesicles [14]. GUV heterogeneity is thought to be due to the inhomogeneous mixing of lipids in the dry film state [15] and the on-going fusion of additional vesicles to form GUVs of unknown compositions [8]. In effect, the irregularities observed across GUVs are inherit to bulk preparation methods which lack precise and immediate control over processes culminating to bilayer formation. Controlling the humidity during lipid film preparation has been reported to ameliorate this problem at the expense of long (24 hr) preparation times [15]. Microfluidics have also helped solve these problems, circumventing the size heterogeneity introduced by GUV electroformation [16,17]. Notably, microfluidics have been recently applied to create phase-separated GUVs using water-in-oil-in-water double emulsions [18]; but these experiments require the fabrication and control of complex devices capable of supporting controlled multiphase flow. Despite these important advances, precise control of bilayer composition remain a significant hurdle to more complex uses of GUVs as mimics of the cell, for example in controlling membrane shape [18–20] and budding in response to changes in the external environment [21,22].

In addition to these unwanted intrinsic changes in membrane composition, intentional changes in composition are also possible: Established methods to induce changes to membrane composition rely on the use of reagents that remove specific bilayer components [6,23,24]. For example, methyl-β-cyclodextrin can be used to modulate the composition of lipid membranes via cholesterol depletion. However, these methods do not enable systematic and precise changes to the composition of lipid bilayers, as the membrane lipid composition after application of these reagents is unknown. Lipid transfer from vesicles to both supported lipid bilayers [25,26] and more recently between GUVs [8] has also been used to modify bilayer composition.

Likewise, Supported Lipid Bilayers (SLBs) have been extensively employed for studying the structural organization of phase-separated mixtures [27?] . However, in contrast to GUVs [9] the surface interactions necessary for SLB formation often result in a reduction in lipid diffusion [28], and immobile domains. Even with polymer cushions, domains are generally immobile [29]. He we exploit the lack of strong substrate interactions in supported Droplet Interface Bilayers (DIBs) to image mobile domains, with lipid diffusion coefficients similar to those observed in free-standing bi-

[a] *Department of Chemistry, University of Oxford, Chemistry Research Laboratory, 12 Mansfield Road, Oxford OX1 3TA, United Kingdom.*
[b] *Department of Chemistry, King's College London, Britannia House, 7 Trinity Street, London SE1 1DB, London, United Kingdom. E-mail: mark.wallace@kcl.ac.uk*
† Electronic Supplementary Information (ESI) available: Supplementary Methods DOI: 10.1039/b000000x/
‡ Present address: Max Planck Institute for Intelligent Systems. Heisenbergstr. 3 70569 Stuttgart, Germany.

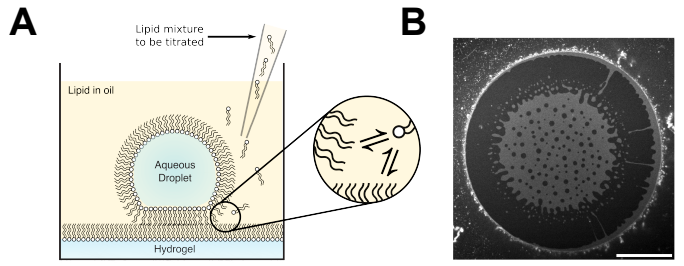

Fig. 1 (**A**) Control of bilayer composition is achieved by titrating lipids into the oil phase. (**B**) Image of a phase-separation in a DIB composed of 1:1:1 DPhPC:DPPC:Chol taken using confocal microscopy. 1 mol% TRITC-DHPE labelled the L_d phase. Scale bar 50 μm.

layers[30].

Here, we exploit the DIB formation process to achieve precise control of the composition of an individual lipid bilayer (**Fig.1**). DIBs are formed in a microfluidic chamber at the contact of a hydrogel-supported lipid monolayer and a second monolayer surrounding an aqueous droplet, both immersed in a lipid-in-oil bath[31]. We originally developed DIBs to provide high-sensitive single-molecule fluorescence imaging of a lipid bilayer whilst retaining control of the membrane potential[32–35]. Unlike GUVs, where changes in lipid mixing can occur as the dry lipid film rehydrates, lipids in DIBs are free to mix both before and after bilayer formation, remaining in equilibrium with the lipids solubilized in the surrounding oil. We reasoned that by adding soluble lipid components to the oil phase surrounding individual DIBs, we might modulate the lipid composition within the bilayer *in situ*, and observe the subsequent changes in lipid phase separation (Fig. 1A).

Experimental

Materials. DPhPC, bSM and Chol were obtained from Avanti Polar Lipids (Alabaster, AL). DiI-C_{18} was obtained from Invitrogen (UK). TRITC-DHPE was obtained from VWR (Germany). Lipids purchased were used without further purification, dissolved in chloroform at 50 mg ml^{-1} and stored at -20°C until use. All other reagents were obtained from Sigma-Aldrich (Missouri, MO).

DIB formation. DIBs were prepared following our previously reported protocol[36]. Briefly, 50 nL droplets of 90 mM 4-(2-hydroxyethyl)-1-piperazineethanesulfonic acid (HEPES) were incubated for 30 minutes in a solution of the required lipids (8.7 mg mL^{-1} total lipids in a mixture of hexadecane and 10% [v/v] Silicone Oil AR 20) to form a lipid monolayer at the oil-water interface. Meanwhile, 140 μL of 0.75% [w/v] low-melt agarose was spin-coated (Laurell Technologies, US) on a plasma-cleaned coverslip at 4000 rpm for 30 s. The agarose-coated cover slip was sealed with a micro-fabricated poly(methyl methacrylate) (PMMA) microfluidic device (details reported previously[36]). Agarose was used to seal the device onto the coated coverslip. The device was filled with the specified lipid solution. After 20 minutes droplets were transferred to the device and bilayers formed upon droplet contact with the agarose substrate. Finally, the device was heated (46°C) above the transition temperature of the lipids used, cooled to room temperature and imaged using

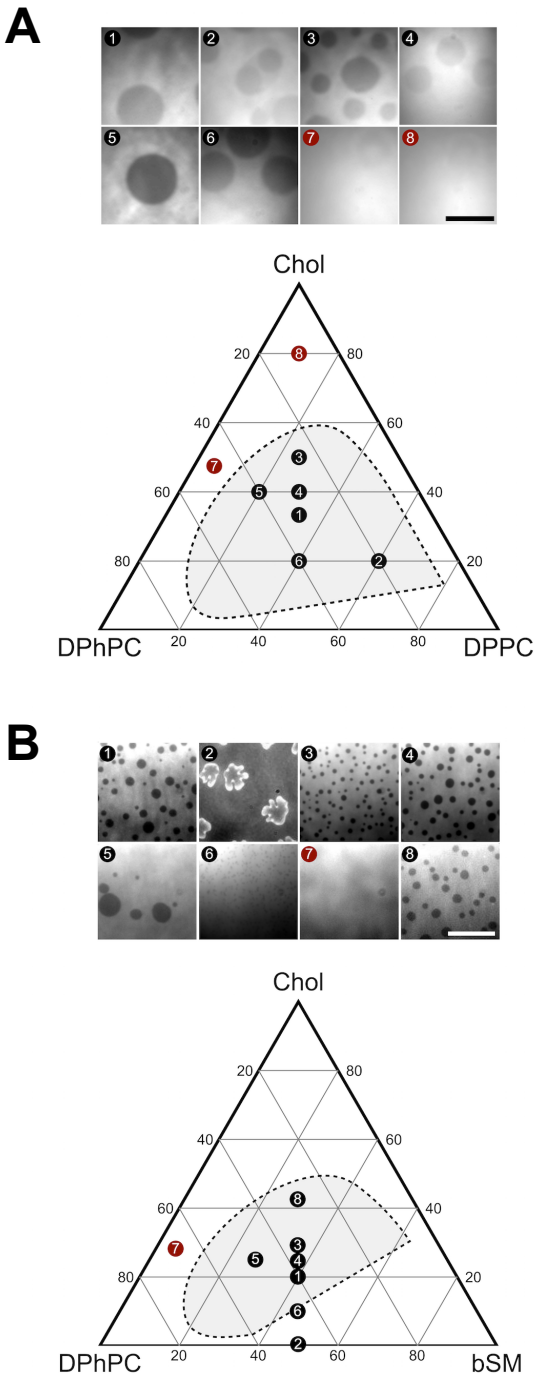

Fig. 2 Sampling of ternary lipid mixtures in DIBs. (**A**) TIRF microscope images of DIBs composed of DPhPC, DPPC and Chol at different molar compositions: (1) 1:1:1, (2) 1:3:1, (3) 5:5:10, (4) 3:3:4, (5) 4:2:4, (6) 4:4:2, (7) 4.75:0.5:4.75, and (8) 1:1:8. (1), (3), (4), (5) and (6) lie in the two-phase region. (2) Lies in the three-phase region. (7) and (8) lie in the single-phase region. Scale bar 5 μm. Phase boundary is reproduced from Veatch et al.[12] (**B**) TIRF microscope images of DIBs composed of DPhPC, bSM and Chol at different molar compositions: (1) 2:2:1, (2) 5:5:0, (3) 1:1:1, (4) 3.75:3.75:2.5, (5) 10:5:5, (6) 9:9:2, (7) 6.25:0.65:3, and (8) 3:2.8:4.). (1), (3), (4), (5), (6) and lie in the L_o/L_d phase coexistence region. (2) lies in the S_o/L_d phase coexistence region. (7) lies in the L_d single-phase region. Phase boundaries are reproduced from Bezlyepkina et al.[8]

TIRF microscopy.

Lipid titration. Solutions of lipids in oil were prepared; the final concentration of lipids in each vial was chosen to maintain the total net concentration of lipids in the device constant. Likewise, the accumulated volume of the individual titrations (600 μL) was chosen so not to exceed the volume of a single microfluidic well (2.5 mL). To achieve a change in bilayer composition, the content of a prepared vial was pipetted into the oil solution contained within the microfluidic device. Immediately following titration the device was heated above the transition temperature of all components (46°C) for 15 minutes and then imaged using TIRF microscopy.

Domain tracking. A custom Matlab (Math Works) script was written to identify domains and measure their size and diffusion parameters. Briefly, a 50% intensity threshold was applied to identify domains. Segmented areas are then isolated based on their size (area $> 0.25\ \mu m^2$) and circularity (i.e. ratio of the major axis length to minor axis length) (rmin/rmax > 0.8). Domains were then tracked by determining their centroid position. Diffusion coefficients were calculated from a weighted least-square fit of the gradient from a plot of the mean square displacements (MSD) versus time. Assuming circular shape, the radius of a domain was then calculated from its area.

MSDs were subsequently analysed as a function of domain radius, r. After comparison of a number of theoretical models[9,37–40], these data were best fit by the Guigas-Weiss model: an empirically-derived fit to the diffusion of different-sized domains in free-standing membranes obtained from molecular dynamics simulations[41]. The fit is mathematically described as:

$$D = \frac{k_B T \arctan(c/r)}{8\eta_w r} \quad (1)$$

Where c is a membrane viscosity-dependant scaling factor, and η_w the bulk viscosity of water.

Results

DIBs containing phase-separating lipid mixtures were prepared following our previously published method[36].

A wide-field confocal image of a representative DIB with liquid-ordered (L_o) liquid-disordered (L_d) phase coexistence is shown in **Fig.1B**. A mixture of 1:1:1 mol% 1,2-diphytanoyl-*sn*-glycero-3-phosphocholine (DPhPC), 1,2-dipalmitoyl-*sn*-glycero-3-phosphocholine (DPPC), and cholesterol (Chol) was used. 1 mol% TRITC-DHPE labelled the L_d phase. Phase-separated DIBs showed essentially consistent domain size and morphology, however near the bilayer edge, where there is contact between bilayer and the two adjoining monolayers on the droplet and agarose substrate, a gradual variation in domain morphology and area fraction was observed.

Focusing on the central region, specific ternary lipid mixtures were sampled to test if compositions where phase-separation has been previously reported for GUVs were also consistent with those we observe in DIBs. **Figure 2** shows phase diagrams and Total Internal Reflection Fluorescence (TIRF) micrographs of DIBs containing different ternary lipid mixtures of either: DPhPC, DPPC, and Chol; or DPhPC, brain-sphingomyelin (bSM) and Chol. 1

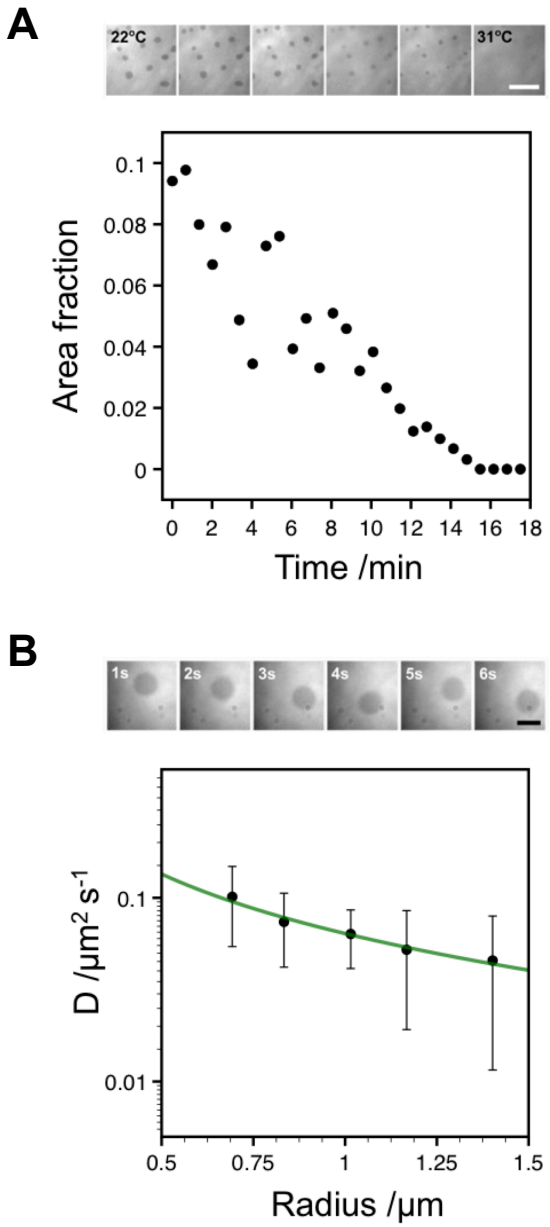

Fig. 3 (**A**) Inset shows an image sequence following heating of a DIB formed from a 1:1:1 DPhPC:bSM:Chol mixture with 1% TRITC-DHPE used as marker for the L_d phase. Heating from 22 (top) to 31°C (bottom) over a period of 5 minutes results in a decrease in L_o area fraction. Scale bar 10 μm. (**B**) Inset shows a 6 s time series of images that show diffusing microdomains. A plot of diffusion coefficient vs. domain radius was fit to the Guigas-Weiss model of domain diffusion ($\chi^2 = 1.329$, $\eta_c = 0.00363$ N s m^2, $c = 6.475 \times 10^{-6}$). Error bars report the standard deviation ($N = 36$). Scale bar 10 μm.

mol% TRITC-DHPE and DiI-C_{18} were used as markers for the L_d phase as indicated[42]. 16 different molar compositions of each mixture were sampled, and single- and two-phase coexistence were observed for compositions where such coexistence was expected.[8,12].

The temperature-dependent depletion of L_o domains in a DIB (1:1:1 DPhPC:bSM:Chol, 1 mol% TRITC-DHPE) (**Fig.3A**) was also exxamined. Domains disappeared as the temperature was increased from 22 to 31°C, consistent with the phase transition temperature of this lipid mixture.

The diffusion of microscopic L_o lipid domains in phase separated DIBs were tracked (**Fig. 3B**). DIBs containing 1:1:1 DPhPC:DPPC:Chol (plus 1 mol% TRITC-DHPE) were formed. Image sequences were analyzed using a custom Matlab script to identify and track domain motion. We found the size-dependent diffusion coefficients for tracked domains were well described by the Guigas-Weiss[41] model for domain motion ($\chi^2 = 1.329$), with membrane viscosity $\eta_m = 1.6$ to 5.6×10^{-9} N s m^{-1}, and solvent viscosity $\eta_c = 0.004$ N s m^{-2}, matching literature reports ($\eta_m = 2.4 \times 10^{-9}$ N s m $^{-1}$ and $\eta_c = 0.001$ to 0.05 N s m^{-2})[9,40]. This suggests that, similar to our previous measurements on lipid diffusion in single-phase DIBs[35], the presence of the underlying hydrogel film does not have any major effects on domain diffusion.

Given the similar phase diagrams, transition temperatures, and domain diffusion to those previously reported, we conclude that lipid domains formed in DIBs are essentially similar to those formed in other artificial bilayers, including GUVs.

We then sought to modulate the lipid composition in individual bilayers. Firstly DIBs composed of 1:1 DPhPC:bSM, were formed and visualized using TIRF microscopy. Here, 1 mol% of DiI-C_{18} was used for visualization of the L_d phase. By titrating solutions of DPhPC:bSM:Chol into the oil phase surrounding the DIB in a series of sequential steps (**Fig.4A**) the composition was varied. This titration was designed to cross phase boundaries and provide visual confirmation of a compositional change in the bilayer. The titer was calculated so that the total concentration of the lipids in the oil phase was kept constant at 8.7 mg mL^{-1}. For the lipid compositions used in this work, DIBs are most efficiently formed, and are optimally stable, at a concentration of 8.7 mg mL^{-1}, Below this optimum, droplet stability decreases, above this concentration, the time required for monolayer assembly increases[36]. Working at the specified concentration ensures a good compromise between stability and equilibration time. The droplets were heated to 46°C and then cooled to room temperature to ensure good mixing of bilayer components before imaging. A second, reversible, titration was also performed (**Fig.4B**), here a DIB at an initial composition of 1:1:1.6 DPhPC:bSM:Chol (again, plus 1 mol% of DiI-C_{18}), was modulated to cross between the two- to single- component regions of the phase diagram by the addition of lipid solutions to the oil phase. We show a total of three transitions across the phase boundary within the same bilayer by sequential addition of solutions of 0:0:1.4, 0.875:0.875:0, and 0:0:2.625 DPhPC:bSM:Chol.

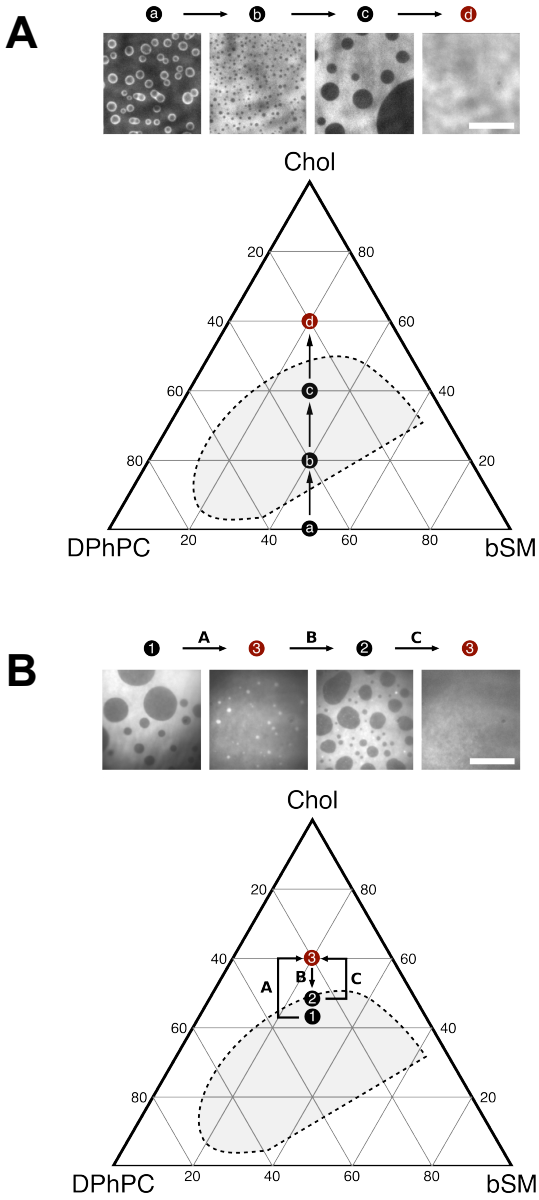

Fig. 4 Control of bilayer composition. (**A**) Titration of cholesterol into a DPhPC:bSM bilayer. (a) lies within the S_o-L_d phase coexistence region. (b) and (c) lie in the two-phase L_o-L_d coexistance region. (d) lies in the single-phase L_d region. Initial molar ratio of lipids at (a) is 1:1:0. Final molar ratio at (d) is 1:1:8. (**B**) Reversible titration of lipids reveals domain switching. Three titrations are performed: (1) to (3), (3) to (2) and (2) to (3). Initial lipid molar concentration, (1), is 1:1:1.6. Final lipid molar concentration, (3), is 1:1:3. Scale bars 17 μm.

Limitations

We note three potential limitations: (1) Our protocol exploited heating of the droplets following each titration; this step can be eliminated, but only at the expense of longer equilibration times; (2) The timescale of composition switching reported here (minutes) is long compared to the timescale of many biological processes; (3) The number of compositional changes must be eventually limited by lipid solubility, although in this work we are well below these limits.

Conclusions

These results show controlled and reversible compositional changes within an individual bilayer. Both the compositions associated with single- and two-phase regions of the phase diagram, and the associated changes in domain area fraction (e.g. 32.4% at (a), 12.6% at (b), 32.8% at (c) and 0% at (d) in **Fig.4A**) are consistent with the phase behavior expected for similar three component lipid mixtures[9,13]. DIB compositions achieved by titration are equivalent to those formed by specific sampling. This can be visually confirmed by comparing points a, b, and c in **Fig.4A** with points 2, 1 and 8 in **Fig.4B**. Within the limits imposed by preparation of specific compositions, and the time required for a composition to equilibrate, the phase behaviour observed for a specific lipid composition is reproducible. State 3 of **Fig.4B** is close to the phase boundary. It is anticipated that the minor differences observed in the images of state 3 are due to systematic errors in the titration of small volumes and the time taken between equilibration and observation. These minor differences are not observed, for example, in **Fig.4A** were the points chosen lie far from the phase boundary and are, thus, less prone to be affected by technical uncertainties. We believe this is a general method of on-demand control of DIB composition. This generality is in contrast to previous reported methods: For example, glycolipid content has been modulated in SLBs[43], however our method is not limited to changes resulting from the action of glycolipid transfer protein; Charged lipids have also been used to achieve vesicle fusion with SLBs[26], however this also places significant restrictions on lipid composition.

This work presents a methodology to systematically modulate the lipid composition of an individual bilayer. Given that DIBs can be used to generate asymmetric bilayers[44], and that a wide variety of complex membrane proteins can be readily incorporated[45], this work provides a route to explore the precise lipid dependence of individual membrane proteins *in situ*. Using DIBs we have shown it is possible to form phase-separated lipid bilayers with precise and homogenous compositions, and to tune the composition of an individual bilayer through direct titration of bilayer components. This tool will be useful in creating more complex mimics of the cell membrane to study phenomena including critical demixing, and protein driven phase separation[10,46].

Acknowledgements

This work was funded by the ERC (CoSMiC). JSHD is supported by a Louis Dreyfus - Weidenfeld scholarship.

References

1 K. Simons and E. Ikonen, *Nature*, 1997, **387**, 569–572.
2 D. A. Brown and E. London, *Annual Review of Cell and Developmental Biology*, 1998, **14**, 111–136.
3 M. A. Alonso and J. Millán, *Journal of Cell Science*, 2001, **114**, 3957–3965.
4 J. Korlach, P. Schwille, W. W. Webb and G. W. Feigenson, *Proceedings of the National Academy of Sciences of the United States of America*, 1999, **96**, 8461–8466.
5 S. L. Veatch and S. L. Keller, *Biochimica et Biophysica Acta (BBA) - Molecular Cell Research*, 2005, **1746**, 172–185.
6 S. L. Veatch and S. L. Keller, *Biophysical Journal*, 2003, **85**, 3074–3083.
7 T. M. Konyakhina, J. Wu, J. D. Mastroianni, F. A. Heberle and G. W. Feigenson, *Biochimica et Biophysica Acta (BBA) - Biomembranes*, 2013, **1828**, 2204–2214.
8 N. Bezlyepkina, R. S. Gracià, P. Shchelokovskyy, R. Lipowsky and R. Dimova, *Biophys J*, 2013, **104**, 1456–64.
9 P. Cicuta, S. L. Keller and S. L. Veatch, *J Phys Chem B*, 2007, **111**, 3328–31.
10 S. L. Veatch, O. Soubias, S. L. Keller and K. Gawrisch, *Proc Natl Acad Sci U S A*, 2007, **104**, 17650–5.
11 S. L. Veatch, P. Cicuta, P. Sengupta, A. Honerkamp-Smith, D. Holowka and B. Baird, *ACS Chem Biol*, 2008, **3**, 287–93.
12 S. L. Veatch, K. Gawrisch and S. L. Keller, *Biophys J*, 2006, **90**, 4428–36.
13 A. R. Honerkamp-Smith, P. Cicuta, M. D. Collins, S. L. Veatch, M. den Nijs, M. Schick and S. L. Keller, *Biophys J*, 2008, **95**, 236–46.
14 J. Larsen, N. S. Hatzakis and D. Stamou, *J Am Chem Soc*, 2011, **133**, 10685–7.
15 E. Baykal-Caglar, E. Hassan-Zadeh, B. Saremi and J. Huang, *Biochim Biophys Acta*, 2012, **1818**, 2598–604.
16 J. C. Stachowiak, D. L. Richmond, T. H. Li, A. P. Liu, S. H. Parekh and D. A. Fletcher, *Proc Natl Acad Sci U S A*, 2008, **105**, 4697–702.
17 D. L. Richmond, E. M. Schmid, S. Martens, J. C. Stachowiak, N. Liska and D. A. Fletcher, *Proc Natl Acad Sci U S A*, 2011, **108**, 9431–6.
18 L. R. Arriaga, S. S. Datta, S.-H. Kim, E. Amstad, T. E. Kodger, F. Monroy and D. A. Weitz, *Small*, 2014, **10**, 950–956.
19 K. Berndl, J. Kas, R. Lipowsky, E. Sackmann and U. Seifert, *Europhys. Lett.*, 1990, **13**, 659–664.
20 K. A. Riske and R. Dimova, *Biophys. J.*, 2006, **91**, 1778–1786.
21 T. Wollert, C. Wunder, J. Lippincott-Schwartz and J. H. Hurley, *Nature*, 2009, **458**, 172–U2.
22 H. Terasawa, K. Nishimura, H. Suzuki, T. Matsuura and T. Yomo, *Proc. Natl. Acad. Sci. U. S. A.*, 2012, **109**, 5942–5947.
23 R. Zidovetzki and I. Levitan, *Biochim. Biophys. Acta-Biomembr.*, 2007, **1768**, 1311–1324.
24 A. Larbi, N. Douziech, A. Khalil, G. Dupuis, S. Gherairi, K. P. Guerard and T. Fulop, *Exp. Gerontol.*, 2004, **39**, 551–558.
25 H. M. Reinl and T. M. Bayerl, *Biochemistry*, 1994, **33**, 14091–

9.
26 A. Kunze, P. Sjövall, B. Kasemo and S. Svedhem, *J Am Chem Soc*, 2009, **131**, 2450–1.
27 S. D. Connell and D. A. Smith, *Molecular Membrane Biology*, 2006, **23**, 17–28.
28 M. Przybylo, J. Sýkora, J. Humpolíčková, A. Benda, A. Zan and M. Hof, *Langmuir*, 2006, **22**, 9096–9099.
29 S. Garg, J. Rühe, K. Lüdtke, R. Jordan and C. A. Naumann, *Biophysical Journal*, 2007, **92**, 1263–1270.
30 A. Sonnleitner, G. Schütz and T. Schmidt, *Biophysical Journal*, 1999, **77**, 2638–2642.
31 H. Bayley, B. Cronin, A. Heron, M. A. Holden, W. L. Hwang, R. Syeda, J. Thompson and M. Wallace, *Mol. Biosyst.*, 2008, **4**, 1191–1208.
32 A. J. Heron, J. R. Thompson, B. Cronin, H. Bayley and M. I. Wallace, *J. Am. Chem. Soc.*, 2009, **131**, 1652–+.
33 L. M. Harriss, B. Cronin, J. R. Thompson and M. I. Wallace, *J. Am. Chem. Soc.*, 2011, **133**, 14507–14509.
34 O. K. Castell, J. Berridge and M. I. Wallace, *Angew. Chem.-Int. Edit.*, 2012, **51**, 3134–3138.
35 J. R. Thompson, A. J. Heron, Y. Santoso and M. I. Wallace, *Nano Lett.*, 2007, **7**, 3875–3878.
36 S. Leptihn, O. K. Castell, B. Cronin, E.-H. Lee, L. C. M. Gross, D. P. Marshall, J. R. Thompson, M. Holden and M. I. Wallace, *Nat. Protoc.*, 2013, **8**, 1048–1057.
37 P. G. Saffman and M. Delbrück, *Proc Natl Acad Sci U S A*, 1975, **72**, 3111–3.
38 E. Evans and E. Sackmann, *J. Fluid Mech.*, 1988, **194**, 553–561.
39 B. D. Hughes, B. A. Pailthorpe and L. R. White, *Journal of Fluid Mechanics*, 1981, **110**, 349–372.
40 E. P. Petrov, R. Petrosyan and P. Schwille, *Soft Matter*, 2012, **8**, 7552–7555.
41 G. Guigas and M. Weiss, *Biophys. J.*, 2006, **91**, 2393–2398.
42 T. Baumgart, G. Hunt, E. R. Farkas, W. W. Webb and G. W. Feigenson, *Biochim. Biophys. Acta-Biomembr.*, 2007, **1768**, 2182–2194.
43 I. Carton, L. Malinina and R. P. Richter, *Biophys. J.*, 2010, **99**, 2947–2956.
44 W. L. Hwang, M. Chen, B. Cronin, M. A. Holden and H. Bayley, *J Am Chem Soc*, 2008, **130**, 5878–9.
45 S. Leptihn, J. R. Thompson, J. C. Ellory, S. J. Tucker and M. I. Wallace, *J Am Chem Soc*, 2011, **133**, 9370–9375.
46 A. R. Honerkamp-Smith, S. L. Veatch and S. L. Keller, *Biochim. Biophys. Acta-Biomembr.*, 2009, **1788**, 53–63.